



Theses and Dissertations

2006-03-16

A multidisciplinary approach to reservoir characterization of the coastal Entrada erg-margin gas play, Utah

Will D. Monn
Brigham Young University - Provo

Follow this and additional works at: <https://scholarsarchive.byu.edu/etd>



Part of the [Geology Commons](#)

BYU ScholarsArchive Citation

Monn, Will D., "A multidisciplinary approach to reservoir characterization of the coastal Entrada erg-margin gas play, Utah" (2006). *Theses and Dissertations*. 371.
<https://scholarsarchive.byu.edu/etd/371>

This Thesis is brought to you for free and open access by BYU ScholarsArchive. It has been accepted for inclusion in Theses and Dissertations by an authorized administrator of BYU ScholarsArchive. For more information, please contact scholarsarchive@byu.edu, ellen_amatangelo@byu.edu.

A MULTIDISCIPLINARY APPROACH TO RESERVOIR
CHARACTERIZATION OF THE COASTAL ENTRADA ERG-
MARGIN GAS PLAY, UTAH

by

Will D. Monn

A thesis submitted to the faculty of

Brigham Young University

In partial fulfillment of the requirements for the degree of

Master of Science

Geology Department

Brigham Young University

April 2006

BRIGHAM YOUNG UNIVERSITY

GRADUATE COMMITTEE APPROVAL

of a thesis submitted by

Will D. Monn

This thesis has been read by each member of the following graduate committee and by majority vote has been found to be satisfactory.

Date

Thomas Morris
Chair, Graduate Committee

Date

John McBride

Date

Bart Kowallis

BRIGHAM YOUNG UNIVERSITY

As chair of the candidate's graduate committee, I have read the thesis of Will D. Monn in its final form and have found that (1) its format, citations, and bibliographical styles are consistent and acceptable and fulfill university and department style requirements; (2) its illustrative materials including figures, tables, and charts are in place; and (3) the final manuscript is satisfactory to the graduate committee and is ready for submission to the university library.

Date

Thomas Morris
Chair, Graduate Committee

Accepted for the Department

Jeffrey Keith
Department Chair

Accepted for the College

Thomas W. Sederberg
Associate Dean, College of Physical and
Mathematical Sciences

ABSTRACT

A MULTIDISCIPLINARY APPROACH TO RESERVOIR CHARACTERIZATION OF THE COASTAL ENTRADA ERG-MARGIN GAS PLAY, UTAH

Will D. Monn

Department of Geology

Master of Science

World-class outcrops of an outermost erg-margin can be observed within the Middle Jurassic Entrada Sandstone near Capitol Reef National Park, Utah. These erg-margin deposits contain isolated reservoir quality sandstone bodies that transition into a muddy tidal flat facies. These high quality reservoirs are dominated by eolian-influenced facies interbedded with sandy interdune facies. They are sealed vertically by muddy and silty facies of associated tidal flat deposits that act as excellent stratigraphic traps in the subsurface. A variety of approaches were used to characterize these Entrada erg-margin reservoirs including: annotated panoramas of outcrops, measured sections, scintillometer measurements of field sections, facies analysis, 2D high-resolution shallow seismic surveys, porosity and permeability analysis, and sedimentary petrography. Logs from the North Hill Creek/Flat Rock gas field were analyzed and correlated to the outcrop study.

Eolian dune facies, along with an upper ripple laminated facies representing interdune deposits, display the highest porosities and permeabilities and are volumetrically the most important facies of the reservoir quality sandstones. Baffles and possible barriers within the sandstone bodies are limited to quartz filled fractures, deformation bands, silty and muddy interdune facies, and first order bounding surfaces.

Many of the sandstone bodies within the outcrop belt are genetically related and in communication with each other. This relationship results from dune complex migration to the south and up section over time. Stratigraphic climb can potentially be imaged seismically and may serve as a key indicator of eolian dune complexes in the subsurface. The volumetric size of one of these complexes is estimated around 470 million cubic feet. Smaller outcrop sandstone bodies were often found to be isolated from the large dune complexes and ranged down to 1 million cubic feet in size.

ACKNOWLEDGEMENTS

This study was funded primarily by the Utah State Geological Survey, Contract # 051844 under the “Characterization of Utah’s Natural Gas Reservoirs and Potential New Reserves” Program, for which I am most grateful. Additional funding was received from the College of Physical and Mathematical Sciences at Brigham Young University. I would like to thank Marc Eckels (VP of Wind River Resources) for his willingness to provide us with well logs as well as other information. Processing and visualization software were donated by Haliburton - Landmark ProMAX2D and Seismic Microtechnology’s Kingdom Suite. Finally, I must thank Thomas Morris, John McBride, and Bart Kowallis whose reviews greatly improved the manuscript.

TABLE OF CONTENTS

TITLE PAGE	i
GRADUATE COMMITTEE APPROVAL PAGE	ii
FINAL READING APPROVAL AND ACCEPTANCE PAGE	iii
ABSTRACT	iv
ACKNOWLEDGEMENTS	vii
TABLE OF CONTENTS	viii
LIST OF TABLES	viii
LIST OF FIGURES	ix
INTRODUCTION	1
METHODS	3
SANDSTONE BODY GEOMETRIES	4
Panoramas and Measured Sections	4
Seismic Survey	9
Rock Body Volumes	13
SAMPLING RESERVOIR QUALITY	14
WELL LOGS	19
Well Log Analysis	19
Outcrop Scintillometer Curves & Log Correlation	20
BARRIERS	22
BAFFLES	24
Faults	24
Fractures	24
Facies and Bounding Surfaces	27
CONCLUSIONS	28
REFERENCES CITED	28

LIST OF TABLES

Table 1: Facies Data

LIST OF FIGURES

Figure 1: Index Map

Figure 2: Erg-Margin Map

Figure 3: Case Study Map

Figure 4: Outcrop Panoramas

Figure 5: Measured Sections Hung from Summerville

Figure 6: Paleocurrent Rose Diagram

Figure 7: Namib Desert

Figure 8: Seismic Line 1

Figure 9: Seismic Line 2

Figure 10: Seismic Line 3

Figure 11: Facies Maps

Figure 12: Measured Sections & Scintillometer Measurements

Figure 13: NHC/FR Field Well Logs

Figure 14: Well Log Correlation to Outcrop

Figure 15: Barriers & Baffles

Figure 16: Photomicrographs

INTRODUCTION

Recent discovery of high btu gas-charged Jurassic Entrada Sandstone reservoirs in the North Hill Creek/Flat Rock (NHC/FR) field located in the southern Uinta basin, Utah have ignited interest in below-Tertiary reservoirs within the basin (Eckels et al., 2005) and possibly in other areas of Utah. Eleven wells in the NHC/FR field have penetrated the productive Jurassic Entrada Sandstone interpreted to be associated with the coastal erg-margin. This interpretation came about from close examination of amplitude time slices from a 3D seismic data set, analysis of the associated well logs, and previous field studies (Marc Eckels, Wind River Resources, personal communication, 2005). Ancient erg-margins are of particular interest because of their potential to contain large, high quality reservoirs. Further, erg-margin sandstones have been recognized as potential stratigraphic and combination hydrocarbon traps especially when they are laterally associated with muddy, marine-influenced facies (Vincelette and Chittum, 1981; Fryberger et al., 1983; Fryberger, 1986; Chan, 1989; Mariño and Morris, 1996). High potential for further development of this play may exist along a north-south trend extending from the Uinta basin through southern Utah.

The Entrada Sandstone was deposited by an extensive erg in the Jurassic (Callovian) Western Interior of the United States (Blakey et al., 1988). Bordering the Entrada erg to the north was a shallow marine sea (Sundance Seaway) while to the west there were sabkha and intertidal mudflats (Kocurek, 1981a). The western erg-margin eolian deposits are commonly found interbedded with marine and mudflat deposits. This western coastal erg facies, as interpreted by Kocurek (1981a), contained simple dunes including small scale irregular crescentic dunes with frequently flooded interdune areas.

The Entrada is widely recognized as an example of a wet eolian system where the water table is close to the surface with the capillary fringe at or near the interdune surface (Kocurek, 1981b; Fryberger et al., 1983; Marzolf, 1988; Carr-Crabaugh and Kocurek, 1998; Mountney, 2004). In these conditions accumulation occurs with rises in the water table and interdunes are susceptible to frequent flooding (Carr-Crabaugh and Kocurek, 1998; Mountney and Jagger, 2004). In the late Callovian and early Oxfordian the Curtis Seaway, an extension of the Sundance Seaway, transgressed over the Entrada erg leaving a simple transgressive erosion surface marked as the J-3 unconformity (Kocurek, 1981a; Caputo and Pryor, 1991; Peterson, 1994).

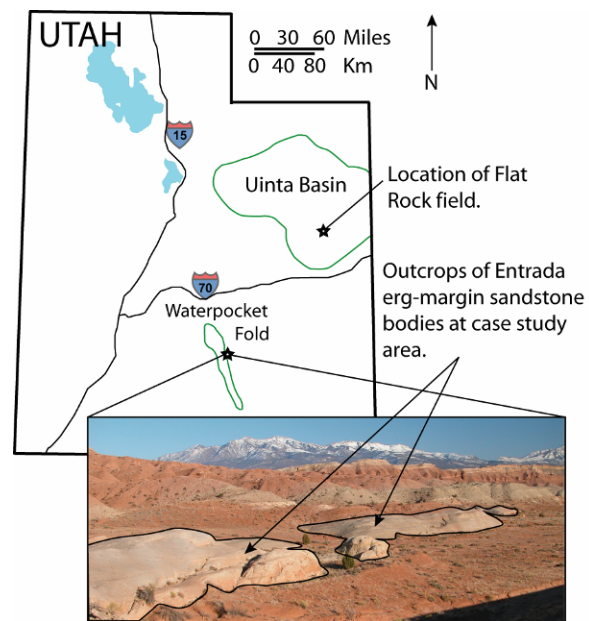


Figure 1. Index map displaying the locations of the NHC/FR field and the case study outcrop.

Entrada erg-margin sandstones exposed in outcrop along the east flank of the Waterpocket Fold near Capitol Reef National Park appear to be isolated sandstone bodies enveloped within an “earthy” facies (Fig. 1). The earthy facies around the sandstone bodies are dominated by dirty sandstones, siltstones, mudstones, and beds of gypsum nodules. Since these outcrops appear to be analogs for reservoirs in the NHC/FR field, they were chosen as a case study area. In order to better constrain the location of this coastal erg-margin, a literature search was completed for articles discussing the location

of the coastal erg-margin trend of the Entrada Sandstone in Utah. Using our own knowledge of the Entrada system and articles from Kocurek (1981a), Eschner and Kocurek (1986), Blakey (1988), Peterson (1988), Anderson and Lucas, (1994), and Peterson (1994), along with the paleogeographic maps they provided, a fairway map was created that approximates the location of the Entrada erg-margin in Utah (Fig. 2).

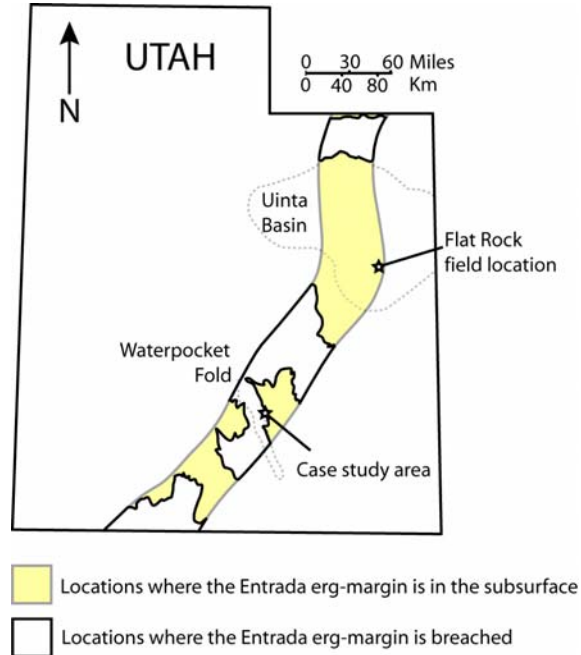


Figure 2. The yellow and white band represents the Entrada erg-margin which has high stratigraphic trap potential. Continuous erg facies of the Entrada lie to the east of the yellow and white band while muddy tidal flat facies lie to the west.

METHODS

Outcrop characterization was initially studied by looking at the sandstone body geometries through panoramas and by measuring stratigraphic sections in 12 locations over the extent of the outcrop. For more information on the sandstone body dimensions, three high resolution seismic reflection surveys were completed in locations where the case study outcrop extended into the subsurface. For reservoir quality information of the outcrop sandstones, facies were closely studied and thoroughly sampled for laboratory analysis. Finally, well log data from the NHC/FR field was examined and compared to data from the case study.

SANDSTONE BODY GEOMETRIES

Panoramas and Measured Sections

First, the 2.5 km outcrop was separated into two fields, labeled as the North Field and the South Field (Fig 3). The North Field consists of six relatively small sandstone bodies that lie

approximately 0.5 km to the north of the South Field, which consists of six relatively larger sandstone bodies.

Panoramas were shot of both the North and South Fields and annotated in order to better understand the

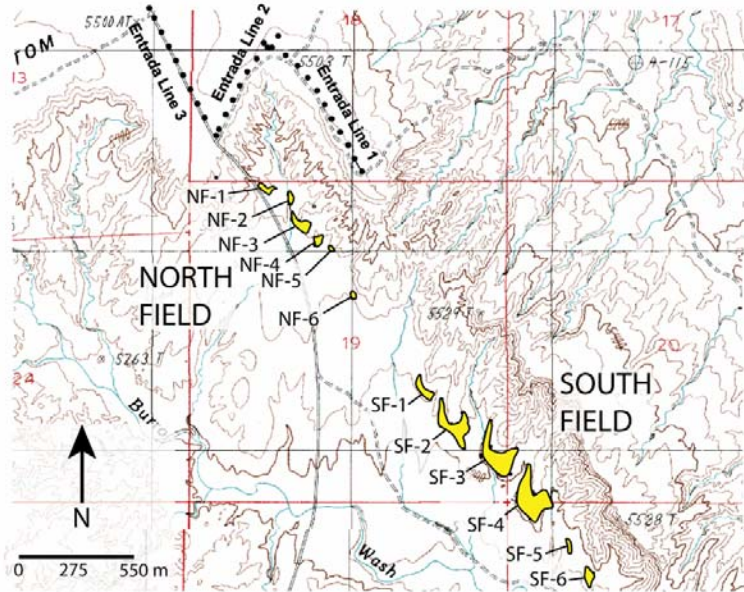


Figure 3. Map showing the case study area and the separation of the two fields along with the sandstone body labels. The locations of the seismic lines are also marked. All strata in the case study area dip approximately 11° NE.

lateral association of the sandstone bodies (Fig. 4). As can be seen on the panoramas, drainages cutting between sandstone bodies are backfilled with alluvium causing the bodies to appear isolated from each other. Though some of the sandstone bodies may be separated stratigraphically from the others, we believe that many of them are actually connected in the subsurface. Due to thicknesses (up to 21-25 m in the South Field) and close lateral proximity of the sandstone bodies, it is very likely that they do connect in the subsurface.

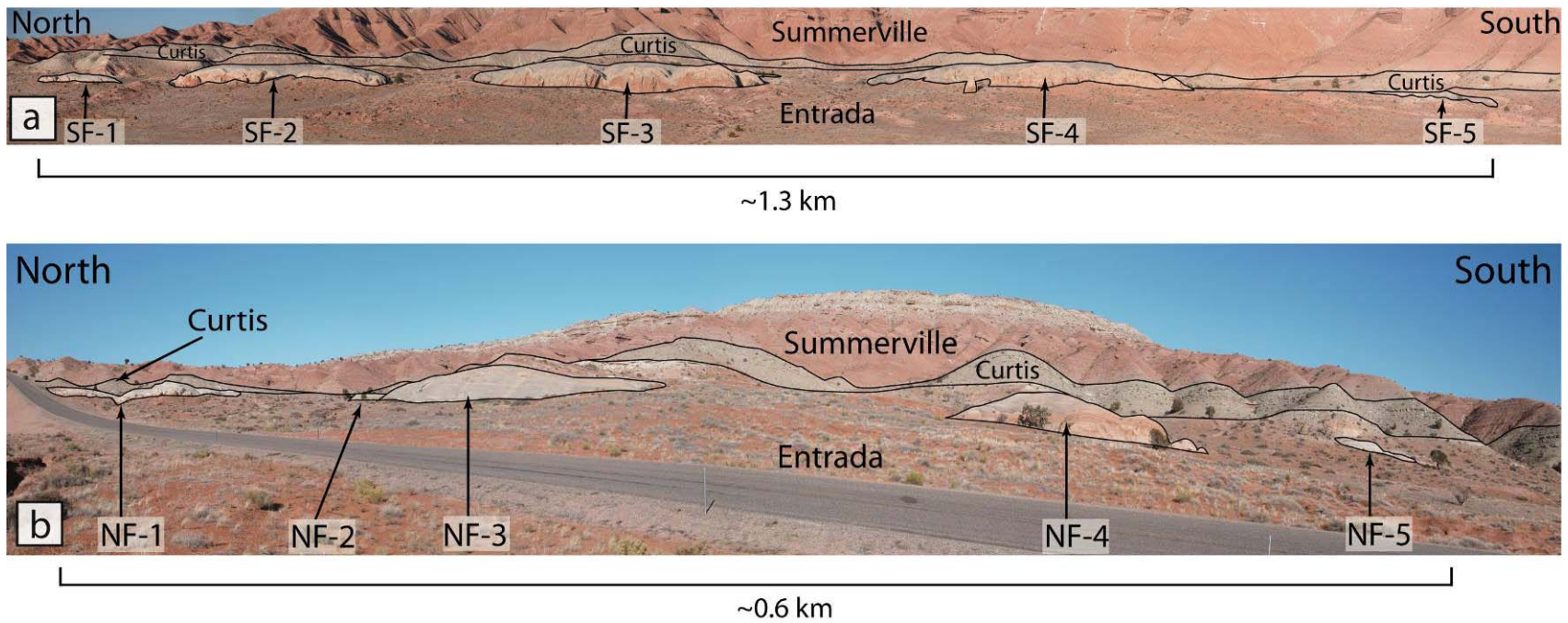


Figure 4. a) Eastward view taken 1 km away from the outcrop. This panorama of the South Field shows five of the six sandstone bodies and their relationships to the overlying Curtis Formation. SF-1 is significantly below the contact while SF-2 through SF-4 become much closer to the contact until SF-5 is actually touching it. b) Eastward view taken 200 m away from the outcrop. This panorama of the North Field shows five of the six sandstone bodies and displays the relationship between the Entrada Sandstone and the Curtis. Note that NF-1 is in contact with the Curtis while the other sandstone bodies are not.

Further, it is apparent that the sandstone bodies become stratigraphically higher to the south. Figure 4a shows that SF-1 and SF-2 are over 15 m below the Curtis Formation-Entrada Sandstone contact while SF-4 and SF-5 are either just below it or right at the contact. To better visualize this relationship, stratigraphic sections were measured from the base of the exposed outcrop of each sandstone body up through the Curtis Formation. Due to the simple transgressive erosion surface (Peterson, 1994) of the Curtis Formation and Curtis contact, the sections were measured up to the Curtis-Summerville contact so that there would be a conformable datum from which the sections could be hung and compared. The completed cross section, Figure 5, better illustrates the stratigraphic relationships of the sandstone bodies by showing their offset and possible correlations.

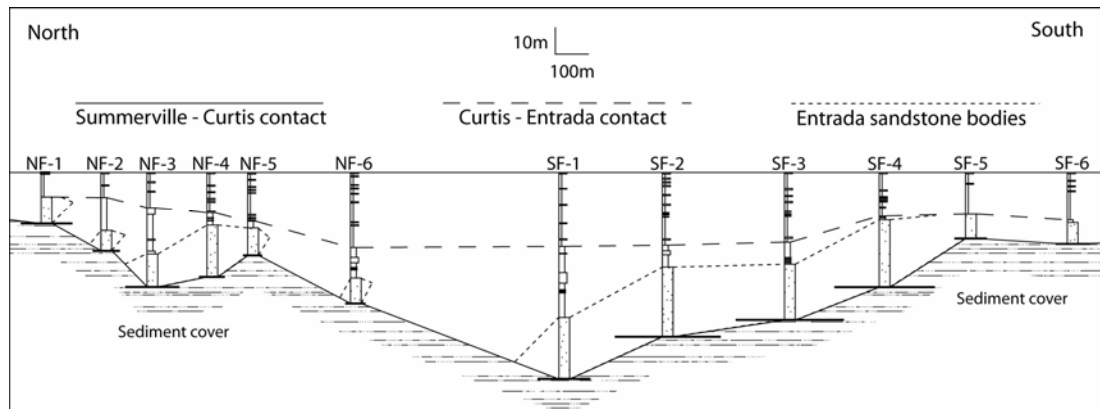


Figure 5. Measured sections hung from the conformable Curtis-Summerville contact. From this figure, the unconformable contact between the Curtis and Entrada can be seen as well as the apparent southward and upward migration of the sandstone bodies. The horizontal lines at the base of each section represent the full surface exposure of each sandstone body. Note that the Curtis sits directly on top of the eolian sandstones in sections NF-1 and SF-5.

Based on our interpretation in Figure 5, we believe that all of the South Field sandstone bodies connect in the subsurface. Because all of the outcrop sandstones have eolian characteristics, with the exception of a few interdune facies, one dune complex initiating near SF-1 and migrating to the south over time could have deposited all of the

outcrops in the South Field. Continuity between sandstone bodies, as described in our interpretation, dramatically increases the reservoir size of the South Field.

The North Field sandstone bodies are notably more isolated than those in the South Field (Fig. 5). In the North Field, several smaller dune complexes are separated from each other. For example, NF-1, NF-2, and NF-6 appear completely disconnected from the other sandstone bodies while NF-3 through NF-5 appear connected. Our seismic interpretation (see below) suggests that NF-1 may also be connected to another southward migrating dune complex at the southern end of seismic Line 3. Thus, similar southward-migrating dune complexes are interpreted to be present both in the North Field and the South Field.

Paleocurrent data also indicates a southeastward wind direction and dune migration pattern (Fig. 6). These measurements were collected from three dimensionally exposed foreset laminations over the extent of both fields and corrected for regional dip using the method given in *Sedimentary Structures* by Collinson and Thompson (1982). Lindquest (1988) details how cross-strata dip direction dispersion patterns can indicate dune morphology, and shows that the pattern we found represents the deposits of a barchan dune. Also using dip direction dispersion patterns, Kocurek (1981a) found that the Entrada erg-margin in northern Utah had crescentic dune morphologies (of which barchans are a subset).

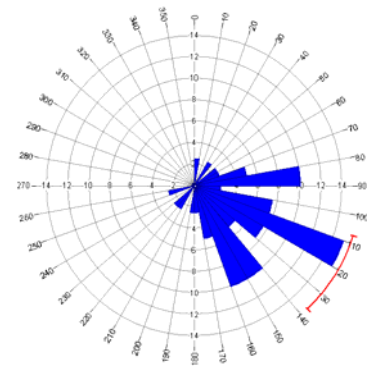


Figure 6. Rose plot of both North and South fields created from 40 data points. The standard deviation is 3.72% with a vector mean of 122.15. Concentric circles represent percent of observations falling into a particular 10 degree bin. Data indicates southeastward dune migration.

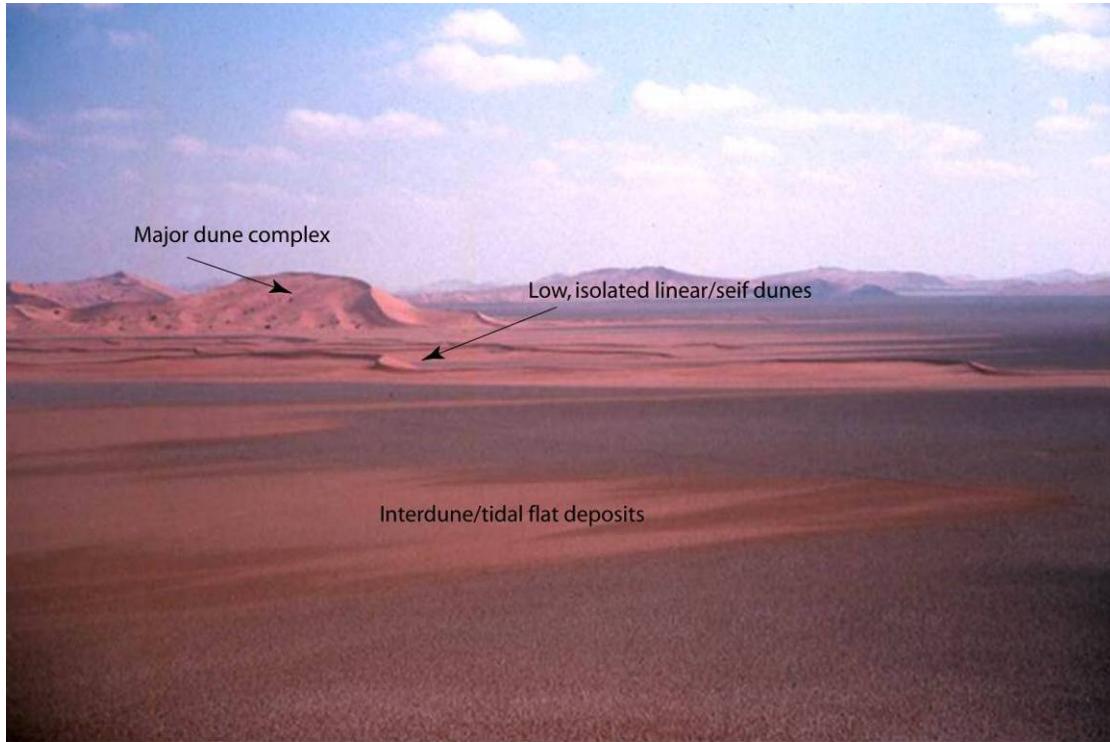


Figure 7. Working depositional model with eolian dunes encroaching on a tidal flat, Namib Desert (taken from Nichols (1979)).

We believe the shoreline of the Namib Desert in South Africa (Fig. 7) is a modern analog to our study area and illustrates what these Entrada erg-margin dune complexes may have looked like during deposition. Using LANDSAT imagery, Lancaster (1983) mapped out dune morphologies in the Namib sand sea. More than 200 km of coastline where found to have crescentic dune morphologies with restricted interdune areas (Lancaster and Teller, 1988) which is similar to what was interpreted in the ancient Entrada coastal erg-margin.

Seismic Survey

From the measured sections and panoramas we obtained good 2D constraints on the geometry and connectivity of the sandstone bodies in both fields. In an effort to obtain a third dimension to the sandstone body geometries, 2D seismic reflection surveys

were shot behind and adjacent to the outcrop where it extends into the subsurface. Three high-resolution compressional wave (P-wave) seismic reflection surveys were shot along and just east of Notom Road where the outcrop dips to the northeast and into the subsurface (Figs. 3). Line 1 (~803 m) was shot along strike on a dirt road on the top of a ridge behind the outcrop while Line 2 (~562 m) was shot on a dirt road that parallels the dip of the outcrop. Line 3 (~584 m), also a strike line, was shot on Notom Road just north of the North Field outcrop. The seismic source used for the acquisition of this data was an ATV-mounted 100-lb accelerated elastic weight dropper (“Seispulse”), field stacked twice. The seismic source and geophone spacing was 10 ft with 48 recording channels giving a nominal fold of cover of 24. Receivers included one 28-Hz geophone per group. A full explanation of the method can be found in *Geophysical Prospecting* by Dobrin and Savit (1988). The data processing includes: trace editing, refraction and elevation statics (datum = 1700 m above sea level), mute, bandpass frequency and dip filtering, deconvolution, normal move-out correction, common midpoint (CMP) stack, depth conversion, and display as color amplitude sections.

Line 1 (Fig. 8) was the first seismic line to be interpreted because accurate stratal thicknesses for the underlying Morrison, Summerville, and Curtis formations could be measured on the slope just below where the line was shot. The Curtis thickness was approximately 5-15 m while the Summerville was approximately 80-90 m thick. Small scale faults within the Summerville section make precise measurement of its thickness somewhat tenuous. We estimate that fault offsets could change the overall thickness by +/- 5-10 m. A thin portion of the Morrison, which lies on top of the Summerville, caps the ridge. Its thickness was found to vary from 1-5 m over the extent of Line 1. Using

measured thicknesses from outcrop; reflectors for each formation were picked and traced over Line 1. Because Lines 1 and 2 intersect near their northern ends, the formation reflectors could be correlated between profiles. Lines 2 and 3 were also correlated even though the southern end of the lines missed crossing each other by approximately 30 m.

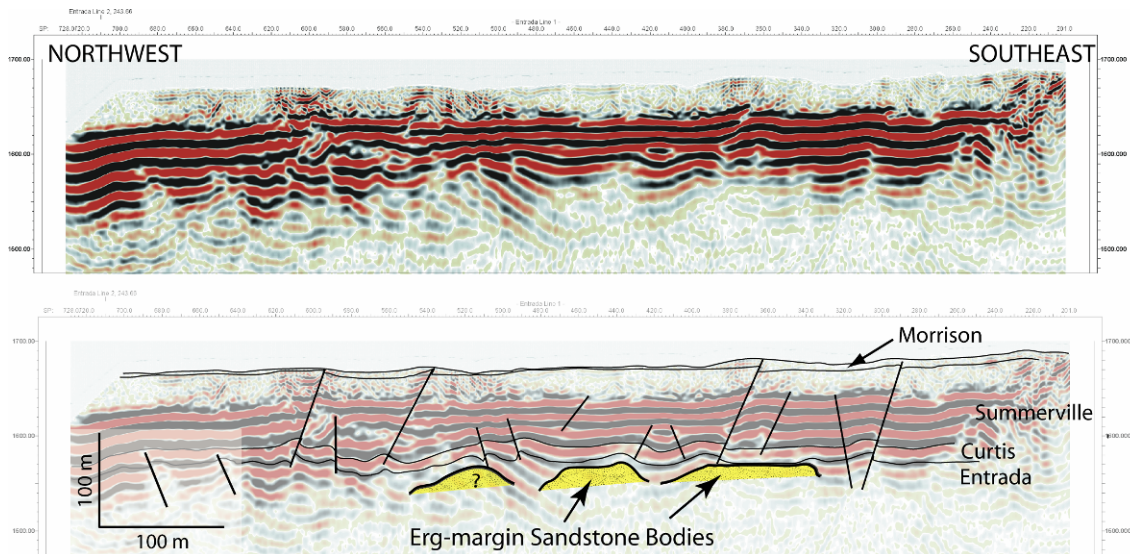


Figure 8. Interpretation of Entrada seismic Line 1.

By looking at the seismic lines it is apparent that seismic resolution deteriorates within the upper Entrada Sandstone which is where we expected to find the sandstone bodies (Figs. 8, 9, & 10). The fading out of the reflectors is attributed to rapid attenuation of the seismic signal by the sandstone bodies. Seismic interpretation of the sandstone bodies was also based upon the relationship of reflectors truncating onto positive features. These areas where there are clear reflectors laterally adjacent to the more “fuzzy” sandstone bodies are interpreted to be onlapping tidal deposits of alternating reworked eolian sands with more silt- and mud-rich sediments. As seen on the interpreted seismic lines and in outcrop panoramas (Figs. 4 & 8), the sandstone bodies

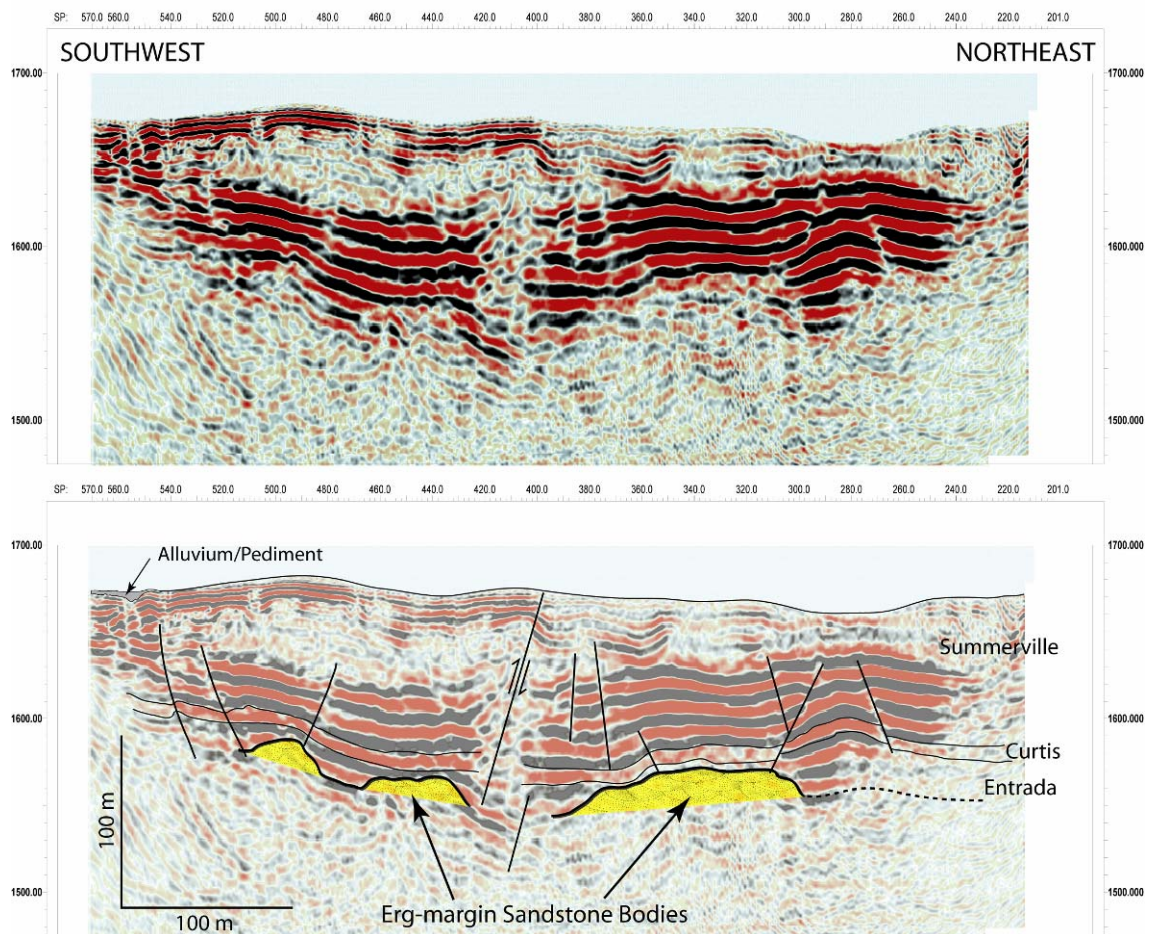


Figure 9. Interpretation of Entrada seismic Line 2.

tend to have flat to rounded tops with an overall dome-like shape. This sort of surficial geometry could be due to erosional relief, reworked relief or inherited relief (original topography). These relationships are commonly found along the Entrada-Curtis contact (Reese, 1981; Vincellette and Chittum, 1981; Fryberger, 1986; Eschner and Kocurek, 1986; Eschner and Kocurek, 1988, and Cheich and Kocurek, 2000) and are discussed thoroughly by Eschner and Kocurek (1986; 1988).

The three seismic surveys indicate that dune complexes continue at least 0.5 km to the north and east. However, in only one case are we able to connect seismically imaged sandstone bodies to those of the outcrop (two sandstone bodies at the southern

end of Line 3 with NF-1; Figure 10). There is the possibility that some of the bodies found in Lines 2 and 3 connect. Both of these lines image bodies with similar morphology and size that are relatively close to each other.

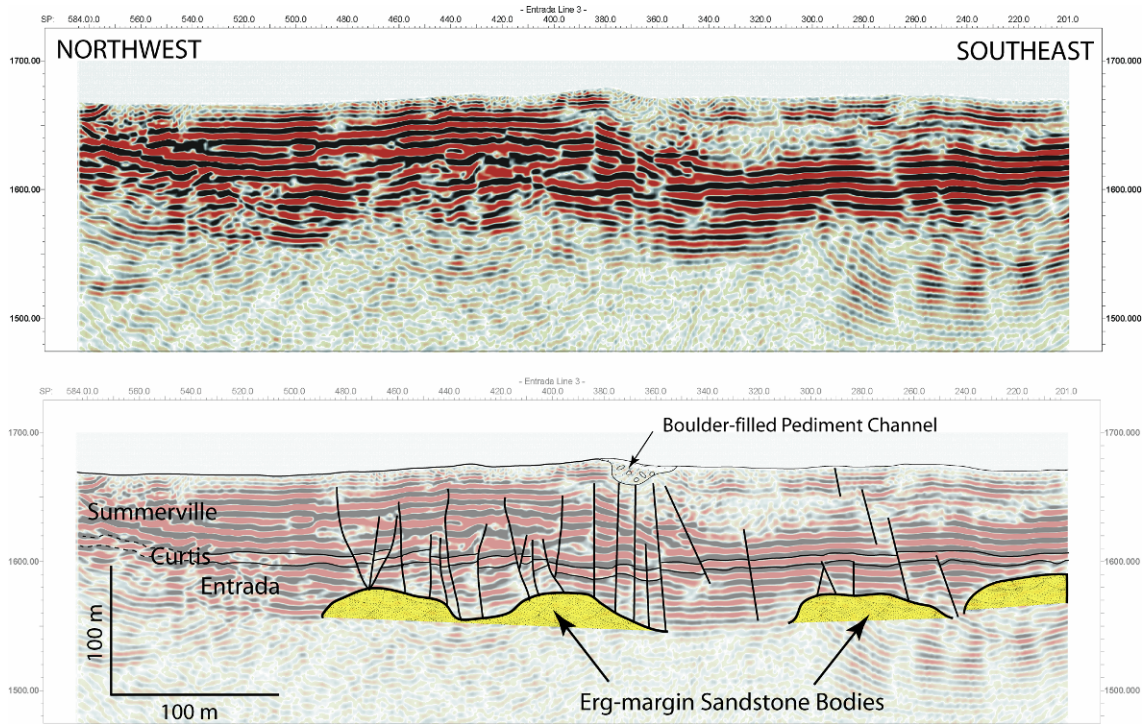


Figure 10. Interpretation of Entrada seismic Line 3. Note the apparent stratigraphic rise of the two sandstone bodies on the southeast end of the survey. The NF-1 outcrop is adjacent to the southeast end of Line 3 and the Curtis Formation sits directly on top of NF-1, suggesting southeastward migration through time.

Rock Body Volumes

High and low estimates of reservoir volumes were calculated based on outcrop measurements. The high case scenario assumes that sandstone bodies SF-1 through SF- 5 are in communication and represent a dune complex. The length of the exposure is approximately 1.3 km, the thickness is an average of the maximum measured thickness of the five bodies (20.5 m), and the lateral extent of the dune complex is estimated at 0.5 km based on the interpretation of sandstone bodies being present in seismic Line 1 (which is set back 0.5 km from the NF exposures). Given the possibility that the sandstone bodies

extend further than 0.5 km into the subsurface, or are thicker in places, the high case scenario could be significantly underestimated. The low case scenario assumes that NF-6 is completely isolated from other sandstone bodies. The length of the exposure is only 28 m, the thickness is assumed to be one half of its maximum thickness (9 m), and the lateral extent into the subsurface is 250 m. The resulting volumes are 470 million cubic feet for the high case scenario and 1 million cubic feet for the low case scenario.

These two scenarios illustrate the high variability of subsurface reservoir size that may be expected in the Entrada erg-margin. Based on outcrop work and 2D seismic interpretation, we suggest that there is a positive relationship between the thickness of a given sandstone body and the potential that it is associated with a large dune complex. The smaller the thickness of a sandstone body, the more likely it is isolated from a large dune complex. Also of note is a thin channel-form sandstone associated within the tidal flat. It is visibly in communication with the NF-1 sandstone body in the North Field and it may connect to other displaced sandstone bodies behind the outcrop. A clean channel sandstone could add significant reservoir volume to these dune complexes.

SAMPLING RESERVOIR QUALITY

Facies were identified and sampled over the extent of the outcrop in order to gain information about the reservoir quality of the rocks being studied. Abbreviations for all of the facies are outlined in Table 1. Not all of the sampled facies are present in both the North and South Fields. The North Field tends to have thinner sandstone bodies, 7.5-12 m thick, and does not display all of the facies found in the South Field. The South Field sandstone bodies are around 21-25 m thick and contain a basal convolute bedding (BCB)

and basal ripple laminated (BRL) facies not found in the North Field. Figure 11 shows the general facies associations found in both the North and South Fields. Two detailed measured sections also show the thickness of each facies along with their relative positions to each other (Fig. 12).

In order to accurately describe and understand these facies, bulk samples were collected from each facies for grain size and thin section analysis. Thin sections were prepared from all of the facies. A 300 point count analysis was completed on each thin section in order to calculate the porosity as a percent, to classify each facies, and to recognize important petrologic features. Core plugs were collected with a 1 inch diameter core drill for porosity and permeability tests. Unfortunately, core plugs were only extractable from the basal ripple laminated facies. These plugs were analyzed with a TerraTek 8400 Dual Porosimeter/Permeameter. Multiple coring attempts from all other facies failed due to the extreme friability of the sandstones. Because of the inability to extract core plugs from other facies, a field mini-permeameter (TinyPerm II Portable Air Permeameter) was used for permeability measurements. These measurements were taken by chipping off the weathered surface of the outcrop and sampling fresh outcrop surfaces. Table 1 summarizes the data collected from the facies sampling.

Table 1. This table displays outcrop and sample analyses completed on each facies. Samples were collected for grain analysis, thin sections, and porosity and permeability tests. Thin section point count porosity values are marked in black while the laboratory calculated values are blue and bold. The laboratory calculated permeability values are also marked in blue and bold while the rest of the values represent field mini-permeameter values. Significant permeability variations were found between measurements taken across laminations and parallel to laminations. All of the higher permeabilities in a particular facies represent ‘parallel to lamination’ measurements. *One exception is the high URL permeability value. This measurement was taken in a highly bioturbated section of the URL facies. It is also important to note that this highly bioturbated URL facies was the ambient rock of the measured cataclasis zone, thus showing a more significant drop in permeability.

Text Abbreviation	Facies	Outcrop Character	Sedimentary Structure	Sorting	Mean Grain Size	Classification	Porosity (%)	Permeability (mD)
MUD	Mudstone	recessive slope former	none visible		mud	mudstone		
BCB	Basal Convolute Bedding	recessive	convolute bedding	moderately well sorted	upper very fine	feldspathic arenite	27.0	455.4
BRL	Basal Ripple Lamination	ledge former	assymetrical ripple lamination, small scale trough cross-stratified sets, soft-sediment deformation, parallel laminations	moderately well sorted	upper very fine	feldspathic arenite	23.9, 25.5, 25.7, 23.7, 24.3	27.5, 264.2, 47.3, 54.3, 265.7, 310.7
SDS	Small Dune Sets	ledge former	<1 meter medium to high trough cross-stratified sets	well sorted	lower fine	feldspathic arenite	26.3	858.12
LDS	Large Dune Sets	ledge former	>1 meter medium to high angle trough cross-stratified sets	moderately well sorted	lower fine	feldspathic arenite	27.7	818.4 perpendicular to foresets, 1218.2 parallel to foresets, 1925.5, 3067.3, 95.5 LDS fracture fill
URL	Upper Ripple Lamination	ledge former, slightly recessive	climbing ripples, symmetrical ripples, soft-sediment deformation, bioturbation, mottled	moderately well sorted	lower fine	feldspathic arenite	26.7	981.6, 969.7, 411.6, *2197.7, 757.7 URL cataclasis zone
UNS	Upper Non-resistant Sandstone	recessive slope former	none visible	moderately well sorted	upper very fine	feldspathic arenite	25.3	1295.5
RLC	Ripple Laminated Channel	ledge former	asymmetrical ripples	moderately sorted	upper fine	feldspathic arenite	18.3	267.3
SILT	Siltstone	recessive slope former	none visible	very well sorted	silt	siltstone	9.3	7.4

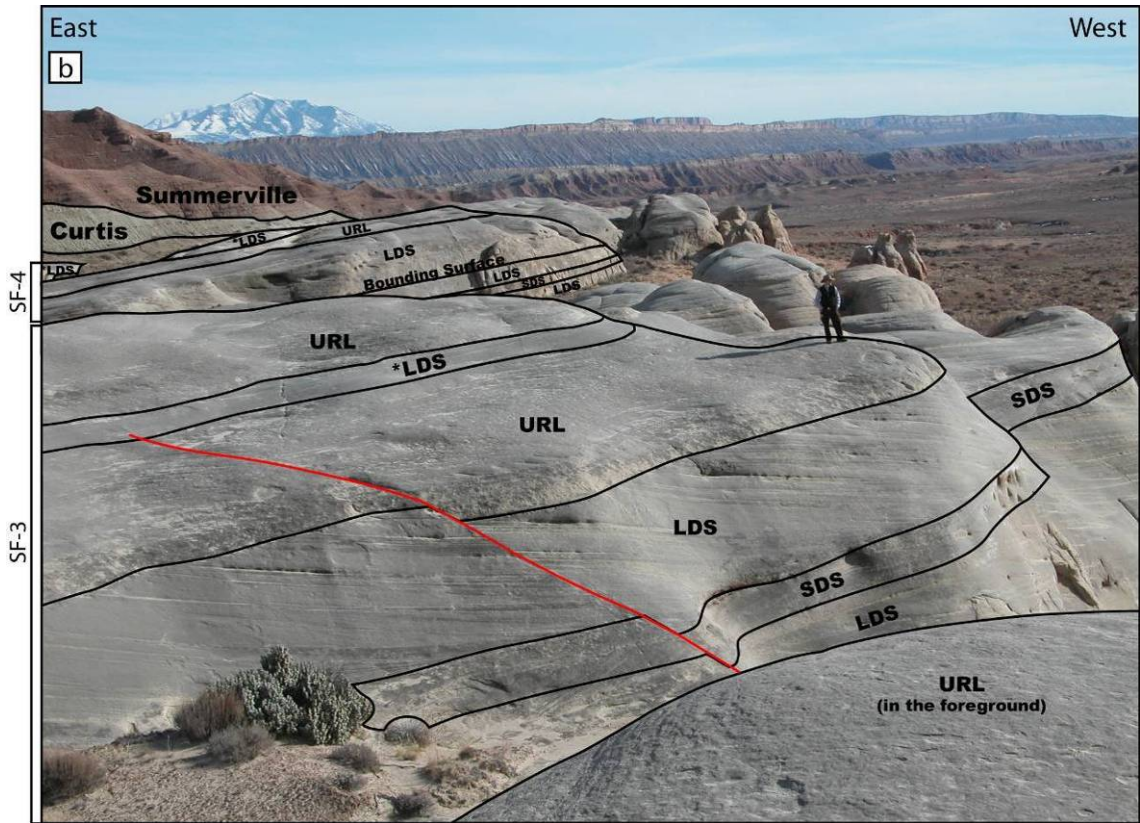
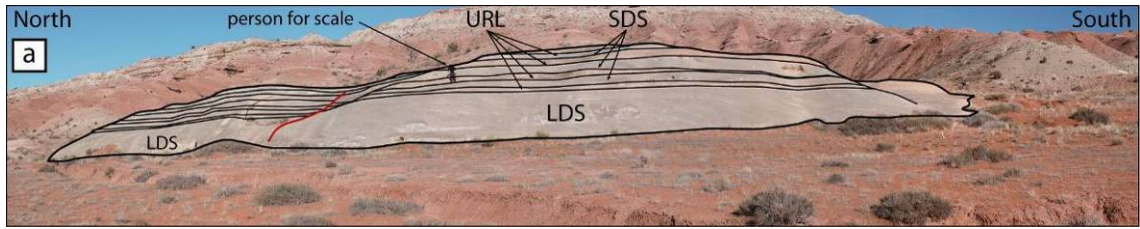


Figure 11. a) Facies relationships commonly found in the North Field with the red line indicating a fault. This photograph is of NF-3. b) Facies relationships commonly found in the South Field. This picture includes SF-3 in the foreground (as well as where the person is standing) and SF-4 in the background. The *LDS represents sections of the LDS facies that were highly scoured.

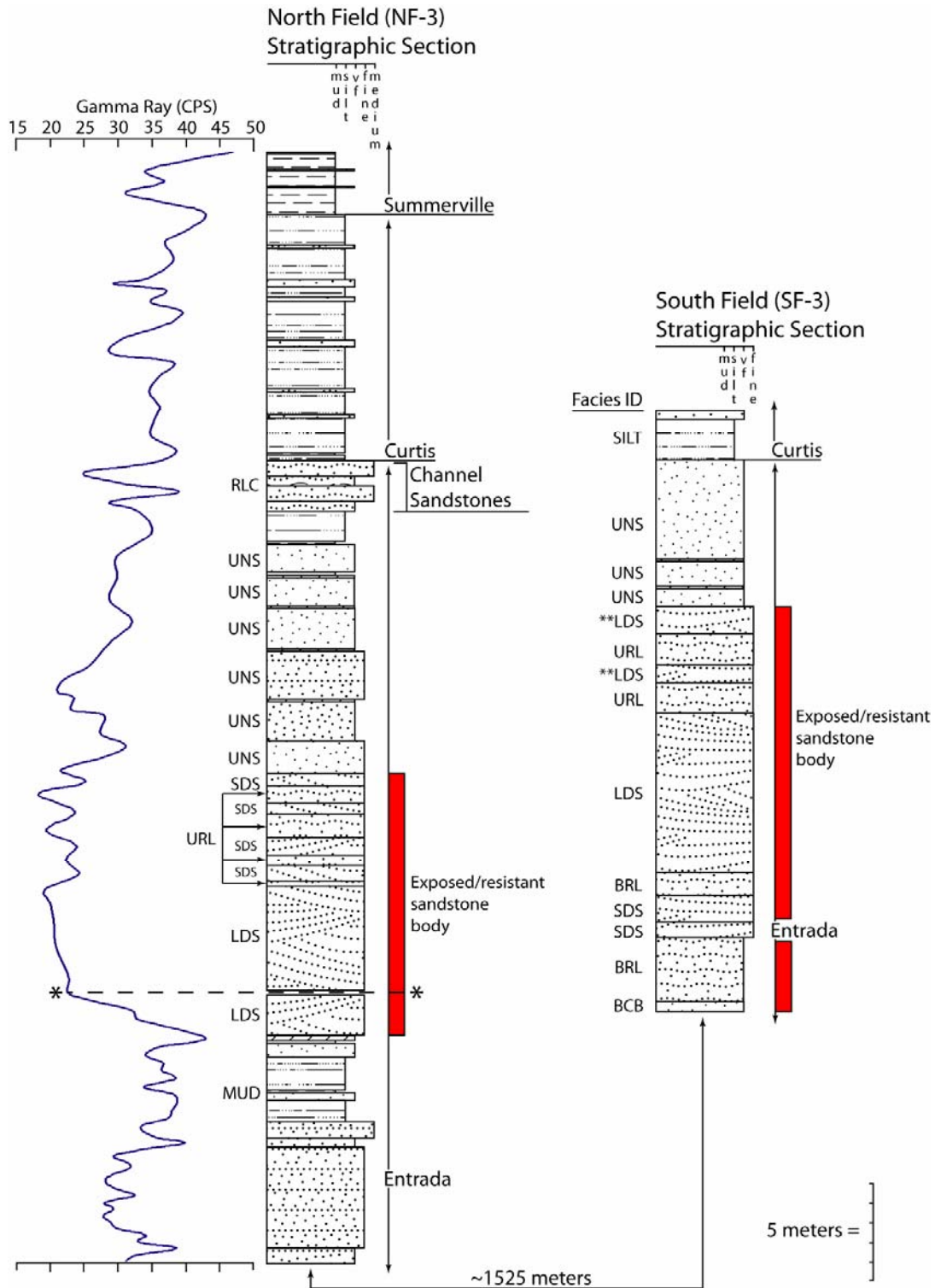


Figure 12. Measured sections and scintillometer measurements of outcrops in the North and South Fields. *Because of the difficulty in finding a portion of the outcrop that exposes the middle, muddier Entrada up through the Summerville, this figure represents a composite measured section. The section above the dashed line was measured where the Curtis-Summerville contact is exposed while the section below it was taken from an outcrop that displayed the muddy portion of the Entrada. Facies are identified on the left side of both sections. The **LDS represents sections of the LDS facies that were highly scoured.

The well log calculated porosity values from the NHC/FR field are significantly less than those found from sample analyses of the case study outcrop. The best Entrada reservoir quality zones of Log 2 have 10.2-12.9% porosities (calculated from density porosity curves) while Log 3 has 14.8-16.1% porosities whereas the majority of the outcrop facies have porosities that range around 23-27%. This variation is primarily attributed to cement reduction from weathering of the exposed outcrop.

WELL LOGS

Well Log Analysis

The NHC/FR field well logs (Fig. 13) show that Entrada sandstones are sealed on the top and bottom by the siltstones and mudstones of the Curtis and Carmel Formations, respectively. Interestingly, the NHC/FR field is producing gas in only certain sections of the Entrada Sandstone. By looking at the gas crossover effect displayed in Figure 13, compartmentalization of the gas-bearing zones is readily notable. It is this relationship, along with the amplitude time slice viewing of 3D seismic data in the NHC/FR field and previous studies that initiated the idea that the productive Entrada sandstones were coastal erg-margin deposits (Mariño and Morris, 1996; Marc Eckels, personal communication 2005).

It is notable that while Log 2 has gas crossover almost throughout the entire Entrada section, Log 3 has crossover in only two smaller zones. The GR curves of Log 2 appear much sandier relative to Log 3. Log 3 likely represents a section with more mudstones and reworked sandstones which would allow for greater compartmentalization of the gas-bearing zones. The variation throughout these well logs is probably due to

their relative position in the erg-margin (whether it is more seaward or landward). The Entrada sections of the case study are best correlated with Log 3, due to the more shale-rich nature of the well log (Fig. 14)

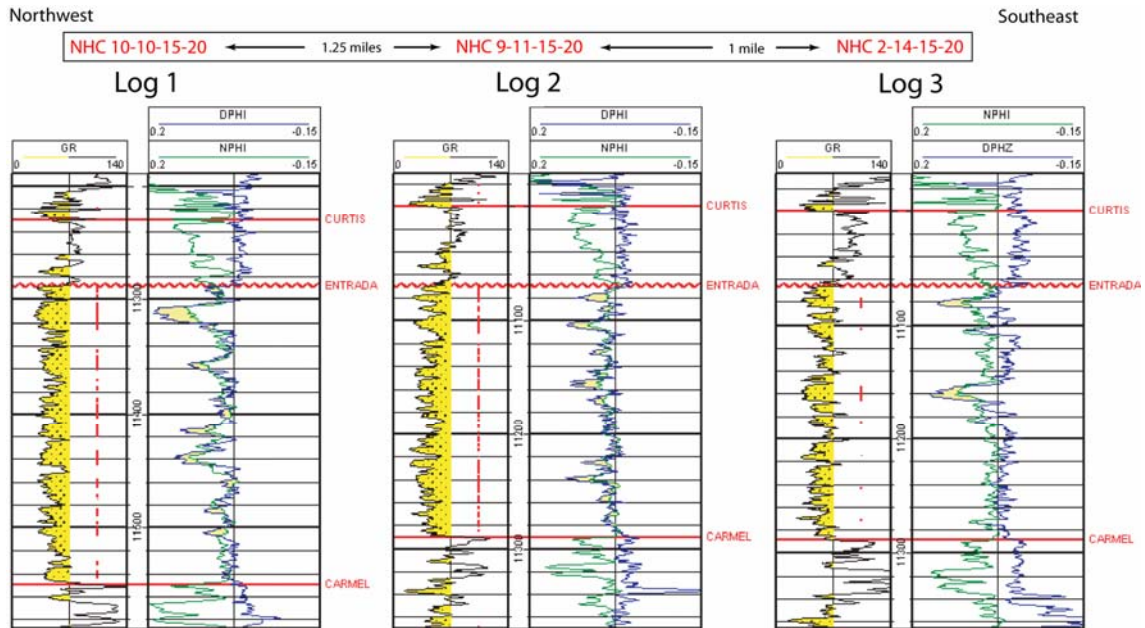


Figure 13. Three well logs from the NHC/FR field that display the entire Entrada section. The logs are hung from the top of the Entrada Sandstone. To better display the muddier intertidal sections on the well logs, all zones between the 70 CPS line and the GR curve were shaded yellow with a sandstone pattern. Neutron and Density Porosity curves were plotted and shaded where they cross to highlight the gas effect. To aid correlation, all gas effect zones were plotted as the vertical red lines to the right of the GR curve seen in Track 1. The shale base-line for Log 1 is ~120 API units, Log 2 ~130 API units, and for Log 3 ~135 API units.

Outcrop Scintillometer Curves & Log Correlation

Scintillometer (gamma ray) readings were taken at approximately 1.5 ft intervals along the same sections of outcrop used for detailed measured sections. These scintillometer readings were plotted as curves and tied to the measured sections so that the outcrop could be better compared to the NHC/FR field well logs (Fig. 14).

The generated scintillometer curve reveals high and low GR kicks within the Entrada (with high kicks occurring in between the clean eolian sandstone bodies) while the Curtis Formation generally displays higher GR kicks. The well logs in the NHC/FR field show a similar response in the Curtis Formation on top of cleaner Entrada Sandstone

with intermittent silty sections marked by higher GR kicks. An apparent difference between the scintillometer curve and Log 1 was the large positive kicks (high GR counts) found in the Entrada section of the outcrop. Log 1 does not display such large positive kicks. However, other well logs, especially Log 3, do show large positive kicks in the Entrada. For example, the high kicks from 11190 to 11200 ft on Log 3 could represent a siltier/muddier section very similar to the ones found in outcrop (Fig. 14). Further, there are several smaller positive kicks in the well logs that mimic the scintillometer GR responses found across the alternating beds of interdune sandstones and cleaner trough cross-bedded sandstones (Fig. 14). We believe most of the smaller GR kicks in Logs 1 and 3 were produced by more silt- and mud-rich interdune deposits.

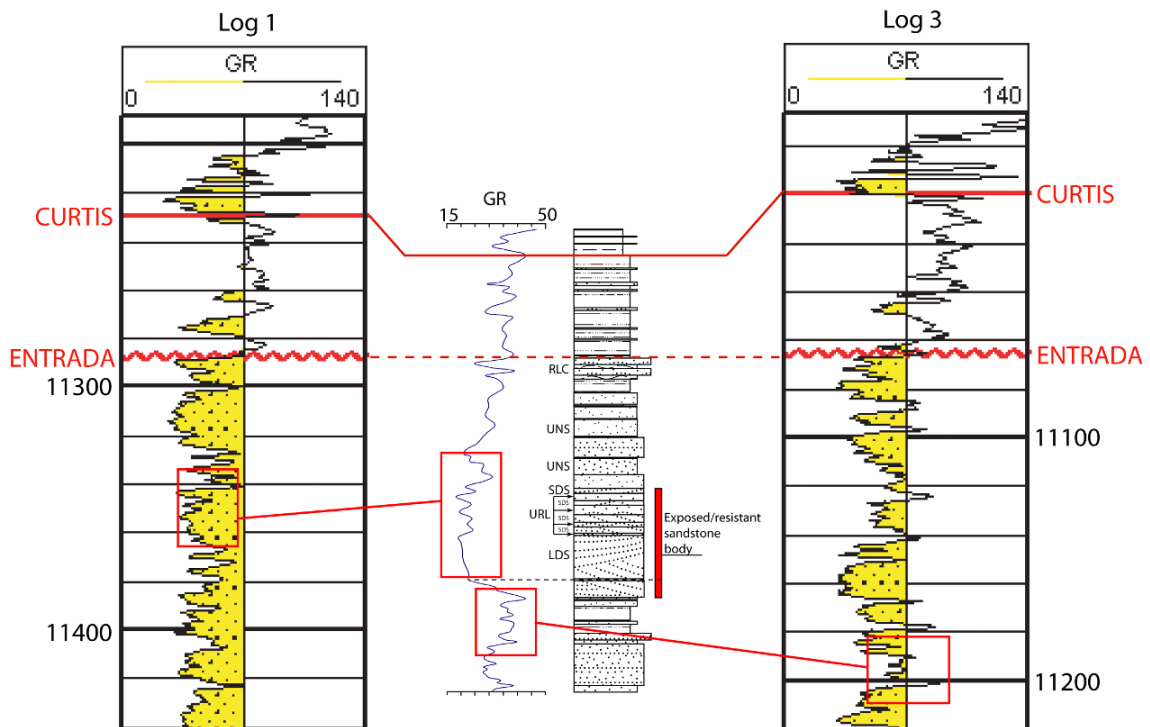


Figure 14. Two well logs are compared to our generated GR curve. All of the curves are hung from the top of the Entrada. The connected red boxes show similar response areas of the well logs and scintillometer curve. The measured section and scintillometer curve are scaled to fit to the well logs which are scaled in feet. The shale base-line for Log 1 is ~120 API units and for Log 3 it is ~135 API units.

Because the NHC/FR field well logs appear to be sandier relative to the case study outcrop, they likely represent a location in the coastal erg-margin that is closer to the erg proper. We expect that the case study outcrop represents a more seaward position on the erg-margin where finer silts and muds could be deposited in the more frequently flooded interdunes. This relationship is visible in Figure 2, with the NHC/FR field being located on the eastern edge of the erg-margin and the case study area towards the center. Because the Entrada is recognized as an example of a wet eolian system where the water table is close to the surface (Kocurek, 1981b; Fryberger et al., 1983; Marzolf, 1988; Carr-Crabaugh and Kocurek, 1998) accumulation and preservation of interdune deposits occur with rises in the water table (Carr-Crabaugh and Kocurek, 1998; Mountney and Jagger, 2004). We speculate that because of the NHC/FR field's close proximity to the main body of this wet eolian system, it had greater sand supply and its preserved interdune deposits were sandier.

With decreased mud and silt intermixed with the sandstones of NHC/FR field, there could still be significant barriers and baffles throughout the Entrada section that would cause compartmentalization. In fact, just below eolian sandstones in the outcrop, water deposited ripple laminated sandstones like the BRL interdune facies have permeabilities up to two orders of magnitude lower than the eolian facies. A drop in permeability, as seen between these facies, may easily produce a baffle in the subsurface.

BARRIERS

Although at least nine facies are recognized within and associated to the eolian-dominated sandstone bodies, the vertical succession of these facies produces no barrier to

fluid flow within the reservoir. Enveloping mudstones, above and below the sandstone bodies, act as excellent hydrocarbon seals (Fig. 15a). In some instances eolian-dominated Entrada sandstone bodies may be in communication with the thin sandstone stringers of the Curtis Formation, but the Curtis sandstone that was sampled gave a low permeability of 1.5 mD. In general, the Curtis Formation, consisting of rippled silty facies deposited on a subtidal to intertidal platform, is overlain and sealed by silt- and mud-rich, restricted, evaporite deposits of the Summerville Formation (Caputo and Pryor, 1991; Anderson and Lucas, 1994).

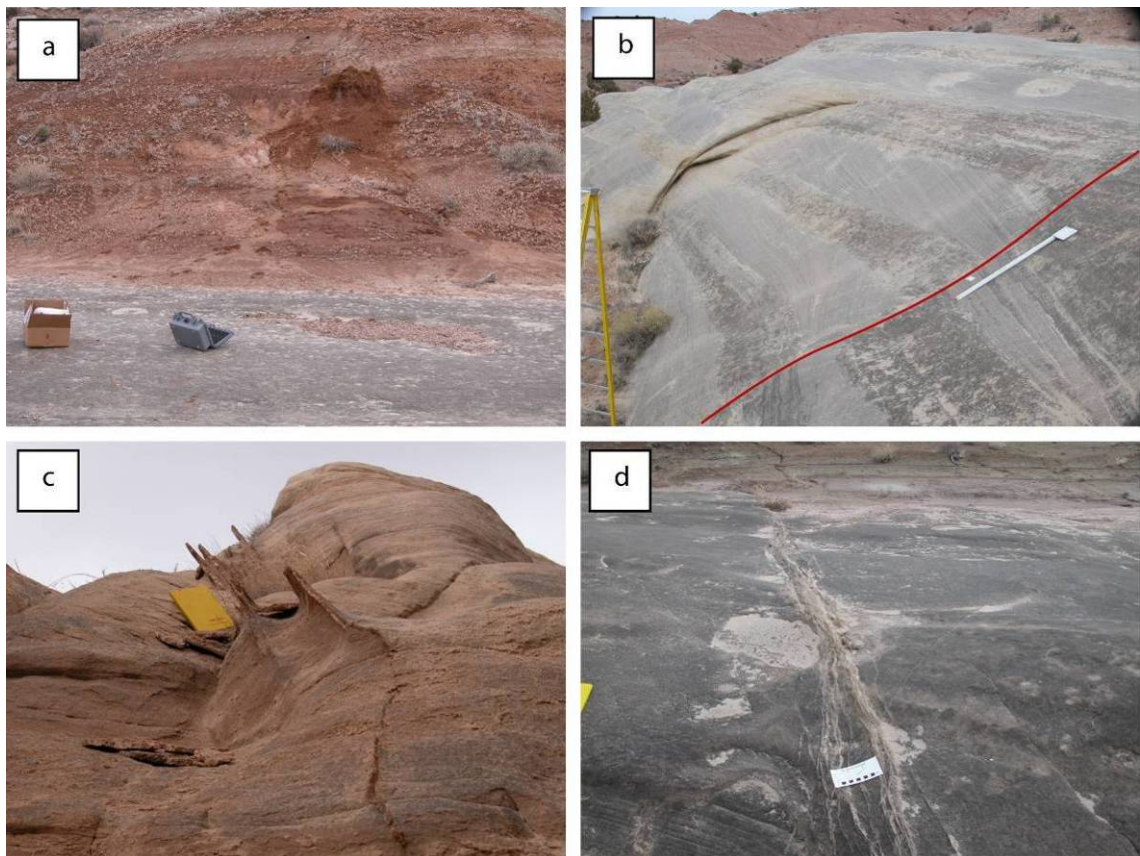


Figure 15. a) Entrada mudstones overlying Entrada reservoir quality, eolian-dominated sandstones. b) A fault with less than one meter of vertical displacement in sandstone body NF-2. 1.5 m jacob staff for scale. c) Differential relief along the quartz-cemented fracture in sandstone body SF-3. d) Deformation bands exhibiting moderate relief. Shearing along these fractures has caused the grains to undergo cataclasis leaving thin bands of much finer grains (Fig. 15b). The throw on the faults are on the order of a few centimeters.

Lateral barriers exist at the edges of the eolian-dominated sandstone “fields” as the sandstones pinchout into tidal flat mudstones and siltstones. However, this may not happen immediately at the edge of the eolian-dominated sandstones as there is some evidence that tide-reworked sandstones exist laterally to the eolian-dominated sandstones.

BAFFLES

Faults

High angle faults exist in the case study sandstones but they have minimal throw (1 m or less) and only extend up to 9 m over the outcrop (Fig. 15b). Close investigation of the fault revealed a sandstone to sandstone contact with little to no visible grain-size reduction or cementation along the fault plane. Because the faults do not cross any argillaceous zones and have sandstone to sandstone contacts, they likely act as fluid conduits rather than baffles or barriers (Gibson, 1994; Antonellini and Aydin, 1995; Garden et al., 2001). However, this is not true of many fractures which leave open the possibility that cementation and deformation bands could potentially baffle or prevent fluid communication across fractures.

Fractures

One fracture was observed in outcrop that is cemented with quartz (Fig. 15c). This quartz-filled fracture stands out in relief relative to the surrounding sandstone and has an average width of 1 cm. The fracture extends obliquely over the extent of the outcrop. The quartz classification is based on the optical properties of the cement as seen in thin section (Fig. 16a) and indicates that the case study sandstones reached burial temperatures up to 80°C where quartz cementation can be reached (Dutton, 1997;

Walderhaug, 1994). In thin section it is obvious that the porosity is reduced but not entirely obliterated. Mini permeameter data revealed a significant decrease in permeability in the fracture relative to the ambient rock. The ambient rock is an eolian facies with permeabilities around 818 mD perpendicular to foresets and 1218 mD parallel to foresets. The permeability taken on the face of quartz-filled fracture only measured as 95.5 mD. These types of fractures undoubtedly act as significant baffles and possibly even barriers at subsurface depths where hydrocarbons may exist.

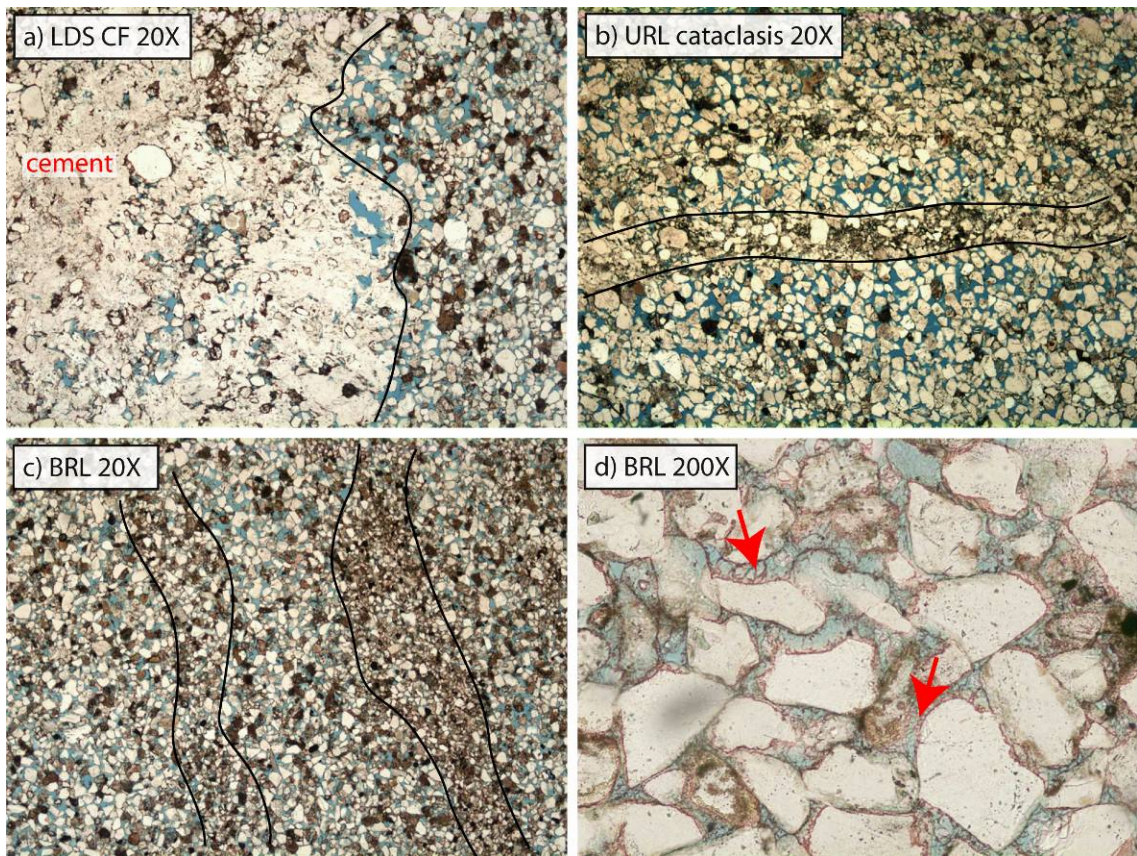


Figure 16. a) View of fracture-fill mineral that has the optical properties of quartz (i.e. uniaxial positive – likely alpha or beta quartz, or even chalcedony). b) View of fractures within the URL facies where cataclasis occurred. c) BRL sandstone with laminae of finer-grained clay-rich sandstone and larger-grained more porous sandstone. d) Red arrows point to some of the clay fibers that bridges between the grains in the clay-rich laminae of the BRL facies.

There are also many deformation band zones over the extent of the outcrop that exhibit moderate relief from the ambient rock. In these fractures the grains have

undergone cataclasis, creating thin bands of silt-sized particles (Figs. 15d, 16b). This cataclasis (grain crushing) typically occurs in porous granular materials and involves porosity collapse and grain fracturing in a tabular zone of localized shear strain (Antonellini and Aydin, 1994; Davatzes and Aydin, 2003; Tindall, 2006). In general, deformation bands are widely recognized as natural barriers to fluid flow causing compartmentalization of reservoirs (Lindquist, 1988, Antonellini and Aydin, 1994 Antonellini, et al, 1994). Many studies have found that deformation bands can reduce reservoir permeabilities from one to three orders of magnitude below that of the matrix (Antonellini and Aydin, 1994; Fowles and Burley, 1994; Garden et al., 2001; Rawling et al., 2001; Sternlof et al., 2004; Tindall, 2006). However, a couple of the studies found that joints cutting across the deformation band zones could connect and allow flow between compartmentalized reservoirs (Davatzes and Aydin, 2003; Tindall, 2006). The bands found in outcrop are 1-2 mm thick and are present in swarms up to 10-15 cm in width that cut vertically across the entire outcrop (without the presence of cross-cutting joints). The total slip along each deformation band is 1-3 cm while over the whole zone the total slip is on the order of decimeters. The outcrop mini permeameter data shows a decrease in permeability across the fracture relative to the ambient rock. In this case, the highly bioturbated ambient rock gave a permeability of 2197.7 mD while the zone of cataclasis measured as 757.7 mD (Table 1). This decrease in permeability is very significant though not enough to create a barrier. However, it is possible that at depth permeabilities could be much lower and flow could be inhibited.

Facies and Bounding Surfaces

Baffles probably do exist within the eolian-dominated sandstone bodies especially when the BRL interdune facies is present. The contact between this facies and those above represents a first-order bounding surface (Kocurek, 1988; Boggs, 2001), which likely acts as a baffle. The BRL facies displays the lowest permeability within the sandstones (varying between bodies 27.5 – 310.7 mD). This reduction in permeability can be attributed to the clay-rich laminae recognized in the thin sections of this facies (Fig. 16c). Ver Hoeve (1982) suggests that clay coatings found in the Entrada developed preferentially in facies where the grains undergo the least abrasion, such as sand sheets and interdunes. The pore spaces within the clay-rich laminae have clay fibers bridging across pores connecting the grains (Fig. 16d). Previous studies on the diagenetic history of the Entrada Sandstone (Ver Hoeve, 1982; Orhan, 1988; Orhan, 1992) indicate that the bridging clay fibers observed are likely smectite and occurred as an early diagenetic phase.

Besides the clay-rich laminae reducing permeability, the facies bounding surface work of Mayo et al. (2003), Holman (2001), and Black (2000) demonstrates that permeability across a facies contact is generally lower than the ambient permeability in either of the facies above or below the contact. One would expect a significant drop in permeability across the contact of two facies even though neither facies is impermeable. Therefore, laterally extensive, horizontal facies contacts may act as baffles to flow. The baffling effect would be more pronounced in reservoirs filled with liquid hydrocarbons than those charged with natural gas.

CONCLUSIONS

Most of the sandstone bodies within the outcrop belt are genetically related and in communication with each other. This relationship results from dune complexes migrating southward and up section through time. Paleocurrent data also shows southward migration of the dunes and indicates that the case study location of the Entrada erg-margin contained crescentic/barchan dune morphologies. Given this type of migration, a single dune complex may vary its stratigraphic level over a 1.3 km field by as much as 30 m. Understanding this type of deposition is crucial in understanding an Entrada erg-margin reservoir and may be a key feature in identifying eolian reservoirs in the outer erg-margin when using seismic.

Eolian dune facies (SDS & LDS), along with the sandier interdune facies (URL), display the highest porosities and permeabilities and are volumetrically the most important facies in the reservoir quality sandstones. Baffles and possible barriers within the sandstone bodies are limited to quartz-filled fractures, deformation bands, silty and muddy interdune deposits (BRL), and first-order bounding surfaces.

REFERENCES CITED

Anderson, O.J., and Lucas, S.G., 1994, Middle Jurassic stratigraphy, sedimentation and paleogeography in the southern Colorado Plateau and southern High Plains. In: Mesozoic Systems of the Rocky Mountain Region, USA (Eds. M.V. Capo, J. Peterson and K.J. Franczyk), Soc. Econ. Paleont. Miner., Rocky Mountain Section, 299-314.

- Antonellini, M., and Aydin, A., 1994, Effect of faulting on fluid flow in porous sandstones; petrophysical properties: AAPG Bulletin, v. 78, p. 355-377.
- Antonellini, M., Aydin, A., and Pollard, D.D., 1994, Microstructure of deformation bands in porous sandstones at Arches National Park, Utah: Journal of Structural Geology, v. 16, p. 941-959.
- Antonellini, M., Aydin, A., 1995, Effects of faulting on fluid flow in porous sandstones: geometry and spatial distribution: AAPG Bulletin, v. 79, p. 642-671.
- Black, B.J., 2000, Fluid flow characterization of the Castlegate Sandstone, southern Wasatch Plateau, Utah: Interpretation of reservoir partitioning through permeability and porosity analysis, M.S. thesis, Brigham Young University, 145 p.
- Blakey, R.C., 1988, Basin tectonics and erg response. In: G. Kocurek (Editor), Late Paleozoic and Mesozoic Eolian Deposits of the Western Interior of the United States: Sedimentary Geology, v. 56, p. 127-151.
- Blakey, R.C., Peterson, F., and Kocurek, G., 1988, Synthesis of Late Paleozoic and Mesozoic eolian deposits of the Western Interior of the United States: Sedimentary Geology, v. 56, p. 3-125.
- Boggs, S., Jr., 2001, Principles of Sedimentology and Stratigraphy, 3rd ed.: Prentice Hall, Upper Saddle River, 726 p.
- Caputo, M.V., and Pryor, W.A., 1991, Middle Jurassic tide- and wave- influenced coastal facies and paleogeography, Upper San Rafael Group, East Utah. In: Geology of East-Central Utah, 1991 Field Symposium, Utah Geological Association Publication, v. 19, p. 9-27.

- Carr-Crabaugh, M., and Kocurek, G., 1998, Continental sequence stratigraphy of a wet eolian system: a key to relative sea-level change. In: Relative Roles of Eustasy, Climate, and Tectonism in Continental Rocks (Eds. K. Shanley and P. McCabe), SEPM Special Publications, v. 59, p. 213-228.
- Chan, M.A., 1989, Erg margin of the Permian White Rim Sandstone, SE Utah: *Sedimentology*, v. 36, p. 235-251.
- Cheikh, A.A.B., and Kocurek, G., 2000, Catastrophic flooding of an aeolian dune field: Jurassic Entrada and Todilto Formations, Ghost Ranch, New Mexico, USA: *Sedimentology*, v. 47, p. 1069-1080.
- Collinson, J.D., and Thompson, D.B., 1982, *Sedimentary Structures*: George Allen & Unwin Ltd, London, 194 p.
- Davatzes, N.C., and Aydin, A., 2003, Overprinting faulting mechanisms in high porosity sandstones of SE Utah: *Journal of Structural Geology*, v. 25, p. 1795-1813.
- Dobrin, M.B., and Savit, C.H., 1988, *Introduction to Geophysical Prospecting*, 4th ed, McGraw-Hill Book Co., New York City, 867 p.
- Dutton, S.P., 1997, Timing of compaction and quartz cementation from integrated petrographic and burial-history analyses, Lower Cretaceous Fall River Formation, Wyoming and South Dakota: *Journal of Sedimentary Research*, v. 67, p. 186-196.
- Eckels, M.T., Suek, D.H., and Harrison, P.J., 2005, New, old plays in southern Uinta basin get fresh look with 3D seismic technology: *Oil & Gas Journal*, v. 103, p. 32-40.
- Eschner, T.B., and Kocurek, G., 1986, Marine destruction of eolian sand seas; origin of mass flows: *Journal of Sedimentary Petrology*, v. 56, p. 401-411.

- Eschner, T.B., and Kocurek, G., 1988, Origins of relief along contacts between eolian sandstones and overlying marine strata: AAPG Bulletin, v. 72, p. 932-943.
- Fowles, J., and Burley, S.D., 1994, Textural and permeability characteristics of faulted, high porosity sandstones: Marine and Petroleum Geology, v. 11, p. 608-623.
- Fryberger, S.G., Abdulkader, M.A., and Clisham, T.J., 1983, Eolian dune, interdune, sand sheet, and siliciclastic sabkha sediments of an offshore prograding sand sea, Dhahran area, Saudi Arabia: AAPG Bulletin, v. 67, p. 280-312.
- Fryberger, S.G., 1986, Stratigraphic traps for petroleum wind-laid rocks: AAPG Bulletin, v. 70, p. 1765-1776.
- Garden, I.R., Guscott, S.C., Burley, S.D., Foxford, K.A., Walsh, J.J., and Marshall, J., 2001, An exhumed palaeo-hydrocarbon migration fairway in a faulted carrier system, Entrada Sandstone of SE Utah, USA: Geofluids, v. 1, p. 195-213.
- Gibson, R.G., 1994, Fault zones seals in siliciclastic strata of the Columbus Basin, offshore Trinidad: AAPG Bulletin, v. 78, p. 1372-1385.
- Holman, L.S., 2001, The effect of parasequence geometry and facies architecture on reservoir partitioning of the Star Point Sandstone, Wasatch Plateau, Utah, M.S. thesis, Brigham Young University, 157 p.
- Kocurek, G., 1981a, Erg reconstruction: the Entrada Sandstone (Jurassic) of northern Utah and Colorado: Palaeogeography, Palaeoclimatology, Palaeoecology, v. 36, p. 125-153.
- Kocurek, G., 1981b, Significance of interdune deposits and bounding surfaces in aeolian dune sands: Sedimentology, v. 28, p. 753-780.

- Kocurek, G., 1988, First-order and super bounding surfaces in eolian sequences – bounding surfaces revisited: *Sedimentary Geology*, v. 56, p. 193-206.
- Lancaster, N., 1983, Controls of dune morphology in the Namib sand sea. In: M.E. Brookfield and T.S. Ahlbrandt (Editors), *Eolian sediments and processes*, v. 38, p. 261-290.
- Lancaster, N., and Teller, J.T., 1988, Interdune deposits of the Namib Sand Sea: *Sedimentary Geology*, v. 55, p. 91-107.
- Lindquist, S.J., 1988, Practical characterization of eolian reservoirs for development: Nugget Sandstone, Utah Wyoming thrust belt: *Sedimentary Geology*, v. 56, p. 315-339.
- Mariño, J.E., and Morris, T.H., 1996, Erg margin and marginal marine facies analysis of the Entrada Sandstone, Utah: Implications to depositional models and hydrocarbon entrapment. In: M. Morales (Editor), *The Continental Jurassic*. Museum of Northern Arizona Bulletin 60, p. 483-496.
- Marzolf, J.E., 1988, Controls on late Paleozoic and early Mesozoic eolian deposition of the Western United States. In: G. Kocurek (Editor), *Late Paleozoic and Mesozoic Eolian Deposits of the Western Interior of the United States: Sedimentary Geology*, v. 56, p. 167-191.
- Mayo, A.L., Morris, T.H., Peltier, S., Petersen, E.C., Payne, K., Holman, L. S., Tingey, D., Fogel, T., Black, B. J., and Gibbs, T.D., 2003, Active and inactive groundwater flow systems: evidence from stratified mountainous terrain: *Geological Society of America Bulletin*, v. 115, p. 1456-1472.

- Mountney, N.P., and Jagger, A., 2004, Stratigraphic evolution of an Aeolian erg margin system: the Permian Cedar Mesa Sandstone, SE Utah, USA: *Sedimentology*, v. 51, p. 713-743.
- Mountney, N.P., 2004, The sedimentary signature of deserts and their response to environmental change: *Geology Today*, v. 20, p. 101-106.
- Nichols, E.T., 1979, Photograph. In: E.D. McKee (Editor), A study of global sand seas: U. S. Geological Survey Professional Paper 1052, 429 p.
- Orhan, H., 1988, Diagenesis of the Entrada Sandstone in Ghost Ranch Area, New Mexico: *AAPG Bulletin*, v. 72, p. 969.
- Orhan, H., 1992, Importance of dust storms in the diagenesis of sandstones; a case study, Entrada Sandstone in the Ghost Ranch area, New Mexico, USA: *Sedimentary Geology*, v. 77, p. 111-122.
- Peterson, F., 1988, Pennsylvanian to Jurassic eolian transportation systems in the Western United States. In: G. Kocurek (Editor), Late Paleozoic and Mesozoic Eolian Deposits of the Western Interior of the United States: *Sedimentary Geology*, v. 56, p. 207-260.
- Peterson, F., 1994, Sand dunes, sabkhas, streams, shallow seas: Jurassic paleogeography in the southern part of Western Interior Basin. In: *Mesozoic Systems of the Rocky Mountain Region, USA* (Eds. M.V. Capo, J. Peterson and K.J. Franczyk), Soc. Econ. Paleont. Miner., Rocky Mountain Section, p. 233-272.
- Rawling, G.C., Goodwin, L.B., and Wilson, J.L., 2001, Internal architecture, permeability structure, and hydrologic significance of contrasting fault-zone types: *Geology*, v. 29, p. 43-46.

- Reese, R.S., 1981, Stratigraphy and petroleum trapping mechanisms of Upper Jurassic Entrada Sandstone, northwestern New Mexico: AAPG Bulletin, v. 65, p. 567.
- Sternlof, K.R., Chapin, J.R., Pollard, D.D., and Durllofsky, L.J., 2004, Permeability effects of deformation bands in sandstone: AAPG Bulletin, v. 88, p. 1315-1329.
- Tindall, S.E., 2006, Jointed deformation bands may not compartmentalize reservoirs: AAPG Bulletin, v. 66, p. 638-639.
- Ver Hoeve, M.W., 1982, Facies-controlled diagenesis and reservoir character, Entrada Sandstone (Late Jurassic), Durango, Colorado: AAPG Bulletin, v. 66, p. 638-639.
- Vincelette, R.R., and Chittum, W.E., 1981, Exploration for oil accumulations in Entrada Sandstone, San Juan Basin, New Mexico: AAPG Bulletin, v. 65, p. 2546-2570.
- Walderhaug, O., 1994, Temperature of quartz cementation in Jurassic sandstones from the Norwegian continental shelf – evidence from fluid inclusions: Journal of Sedimentary Research, v. A64, p. 311-323.